JACS
JOURNAL OF THE AMERICAN CHEMICAL SOCIETY

Communication

pubs.acs.org/JACS

Synthesis of Surface Covalent Organic Frameworks via Dimerization and Cyclotrimerization of Acetyls

Biao Yang,[†] Jonas Björk,[‡] Haiping Lin,[†] Xiaoqing Zhang,[†] Haiming Zhang,[†] Youyong Li,[†] Jian Fan,[†] Qing Li,*[,†] and Lifeng Chi*[,†]

[†]Jiangsu Key Laboratory for Carbon-Based Functional Materials & Devices, Institute of Functional Nano & Soft Materials, Soochow University, Suzhou 215123, PR China

[‡]Department of Physics, Chemistry and Biology, IFM, Linköping University, 58183 Linköping, Sweden

Supporting Information

ABSTRACT: The formation of additional phenyl rings on surfaces is of particular interest because it allows for the building-up of surface covalent organic frameworks. In this work, we show for the first time that the cyclotrimerization of acetyls to aromatics provides a promising approach to 2D conjugated covalent networks on surfaces under ultrahigh vacuum. With the aid of scanning tunneling microscopy, we have systematically studied the reaction pathways and the products. With the combination of density functional theory calculations and X-ray photoemission spectroscopy, the surface-assisted reaction mechanism, which is different from that in solution, was explored.

The concept of on-surface synthesis, by which well-defined robust molecular structures can be prepared on surfaces via covalent connections, has acquired much attention in recent years[1−11] because it facilitates efficient charge transport and high thermal stability.[12] To date, the most commonly used surface reaction is Ullmann coupling between aryl halides on various noble metal supports.[2,13] With this approach, among other materials,[8] graphene nanoribbons with controlled size and shape have been successfully synthesized.[14−17] Besides the Ullmann coupling, halogen-free reactions were also developed, such as the aryl−aryl direct polymerizations,[9] homocoupling of terminal alkynes,[18−20] cyclodehydrogenation,[21,22] and acylation.[4] Moreover, on-surface chemistry enables reactions that are not possible in solution. For example, a linear alkane polymerization was recently reported via C−H activation on a reconstructed Au(110) surface.[23]

On the basis of the development of on-surface chemistry, various functional networks have been constructed. In particular, two-dimensional (2D) covalently bonded polymers have acquired specific interests because of their similarity to the graphene sheet, with prospects to exhibit novel properties. Normally, 2D covalent networks were obtained on surface via the direct Ullmann coupling[8] of two adjacent monomers or a condensing reaction.[24,25] Very recently, a new protocol for synthesizing 2D porous networks was proposed by aryl alkyne cyclotrimerizations on metal surfaces.[26,27] Cyclotrimerization reactions are seldom reported to construct 2D materials on surfaces under ultrahigh vacuum (UHV), although they have been extensively utilized in the building of covalent organic frameworks (COF) materials in solutions.[28,29]

Herein, we present a new type of surface-assisted chemical reaction, which produces 2D covalent networks by forming an additional phenyl ring through cyclotrimerization of acetyl-containing compounds (Scheme 1). The synthesized 2D networks are conjugated planar sheets built by sp^2-hybridized C atoms. Using scanning tunneling microscopy (STM), we have observed rich polymer products, providing detailed information about the reaction pathways on the Ag(111) surface, involving dimerization (Scheme 1a) and cyclotrimerization coupling (Scheme 1b) of acetyls. Aided by density functional theory (DFT) calculations, we explore plausible reaction mechanisms, discriminating the rate-limiting steps of the reaction and possible side products. The different pathways proposed by DFT can be distinguished by X-ray photoelectron spectroscopy (XPS) experiments. Notably, although acetyl cyclotrimerization is well-known in solution,[30,31] to the best of our knowledge, our attempts are the first report on surfaces under UHV. Therefore, our protocols to form 2D conjugated porous polymer not only contribute to material science but also provide a valuable extension to the on-surface synthesis toolbox.

Scheme 1. Schemes of the Anticipated Reaction Pathway, Illustrating (a) the Dimerization Coupling of Two Acetyls and (b) the Successive Cyclotrimerization Coupling of Acetyls

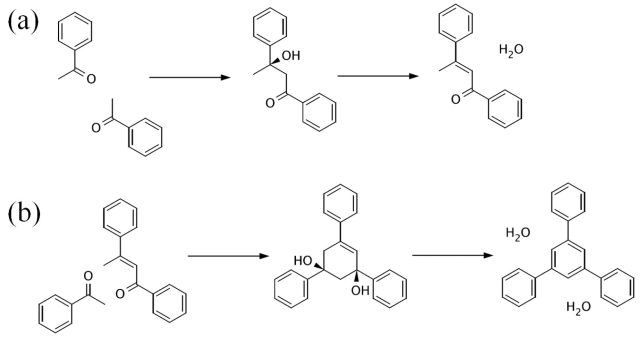

Received: January 23, 2015
Published: March 24, 2015

DOI: 10.1021/jacs.5b00774
J. Am. Chem. Soc. 2015, 137, 4904−4907

Figure 1a gives a representative high-resolution STM image after initial deposition of the precursor molecule 1,3,5-tris(4-acetylphenyl)benzene (TAPB, structural model is shown in the inset of Figure 1a) with the Ag(111) substrate held at room temperature. Individual molecules are clearly distinguished from the image, suggesting that the molecules are not polymerized after room-temperature adsorption. DFT calculations of the supramolecular phase reveal that the molecules land with a planar configuration, and the pinwheel assembly structure is stabilized by the hydrogen bonding between the O atom of the acetyl and the phenyl ring (Figure 1b). In comparison to Au(111) and Cu(111), the STM images on Ag(111) often show fuzzy signals, indicating a relatively weak interaction between the molecules and the substrate (Figure S1).

Normally, chemical reactions can be triggered by either annealing the sample from the initial deposition or depositing organic molecules with the substrate maintained at elevated temperatures. However, we noticed that high-temperature annealing is always accompanied by molecular desorption, making it difficult to control the coverage. Therefore, the latter method was used throughout this study if not mentioned otherwise.

Distinct features were observed after depositing TAPB with the substrate held at 590 K (Figure 1c). The islands are of identical height, with the molecules showing very small lateral irregularities, suggesting phenyl rings oriented parallel with the surface. Closer inspection of the STM images (Figure 1d,e) reveals that the irregular structure consists of porous networks with zigzag edges. Moreover, one can identify that the electron density of the supramolecules is quite smooth with individual monomers indiscernible, which is rather different from that of materials prepared at RT. We naturally attribute the abundant porous features to the supramolecules newly formed by surface-assisted thermally activated chemical reactions.

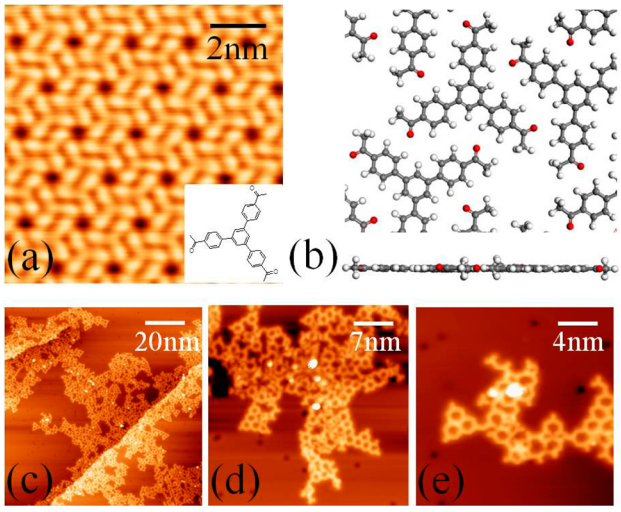

Figure 1. Structural evolution upon the increase of the substrate temperature. (a) STM image after room-temperature deposition. The inset gives the structural model of the TAPB molecules. V_b = 0.5 V and I_t = 50 pA. (b) The top (upper) and side (lower) view of the relaxed model of the self-assembly structure depicted in a. (c) Representative STM image after deposition with the substrate held at 590 K. (d and e) Magnified images of c. The scanning parameters of c to e are V_b = 1 V and I_t = 20 pA.

To further study the reaction, three representative STM images of the products were selected (Figure 2). In Figure 2a, a hexagonal pore is formed via the aggregation of three TAPB precursors. Each precursor has two of their acetyl terminals merged with their adjacent molecules, giving rise to the zigzag edges. This phenomenon agrees well with Scheme 1a in that two acetyl terminals react with each other, resulting in a covalently bonded dimer (highlighted in red, Figure 2d). Figure 2b, however, gives an extended pyramidlike island involving 10 molecules. Similarly, the edge of the island exhibits a zigzag shape, indicating the dimerization coupling of adjacent acetyls. However, in the inner island, three monomers have their acetyl terminals pointing together, giving rise to the cyclotrimerization coupling (Scheme 1b) of the trifunctional acetyl compounds (newly formed phenyl ring highlighted in blue, Figure 2e). One could immediately notice that the dimerization coupling of acetyls only occurs at the border of the nanoisland, whereas the cyclotrimerization coupling of acetyls yields at the inner, which is essential to the formation of extended porous networks. Note that the porous structure is very similar to graphene networks, with the C−C unit in graphene replaced with phenyl−phenyl−phenyl component. To verify our model, we measured the size of the nanostructures (Figure S2). The pore-to-pore distance is 14.9 ± 0.2 Å, in excellent agreement with the calculated value of 15 Å. Notably, the pore-to-pore distance is 0.7 and 0.75 nm, respectively, of the previously reported porous graphene prepared via Ullmann coupling.[8,32] In addition to the porous structure, one could also observe the extended sections of zigzag edges (Figure 2c,f), again validating the dimerization coupling of adjacent acetyls. We have carefully measured the size of various types of products, as shown in Figure S2, which are in nice agreement with the experimental results, thus unambiguously verifying our proposed structural model. Notably, for alkyne cyclotrimerization two regioisomers can be formed: the 1,3,5- and 1,2,4-trisubstituted benzene rings.[27] Our protocols, however, provide fairly nice reaction selectivity toward unified 1,3,5-trisusbstituted benzene rings.

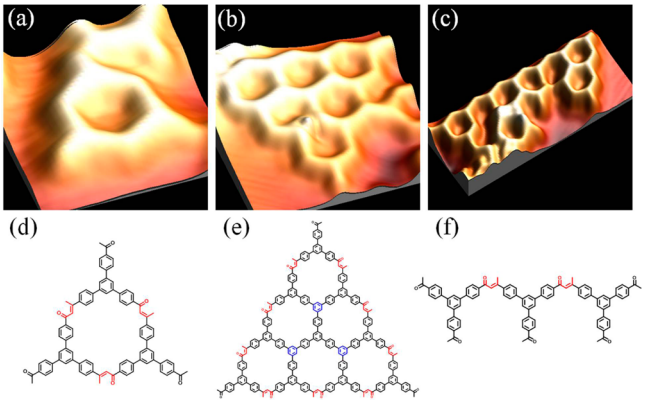

Figure 2. (a−c) Three types of representative reaction products. V_b = 1 V and I_t = 20 pA. Image sizes are 3.7 × 3.7, 6.0 × 6.0, and 10.6 × 4.4 nm^2, respectively. (d−f) Proposed structural models of a−c. Red and blue denote the product of dimerization coupling and cyclotrimerization coupling reaction of acetyls, respectively.

Because the reaction is thermally triggered, the yield rate is sensitive to the substrate temperature during the molecular deposition. Substrate-temperature-dependent studies show that dimerization coupling of acetyls dominates at relatively low temperatures. The number of the additional phenyl rings

DOI: 10.1021/jacs.5b00774
J. Am. Chem. Soc. 2015, 137, 4904−4907

formed through cyclotrimerization coupling of acetyls increases upon the elevation of the substrate temperature (Figure S3).

To further study the process of the surface reaction, periodic DFT calculations were performed using the VASP code.[33] We used the van der Waals density functional (vdW-DF)[34,35] in the recent form by Hamada,[36] which was shown to accurately describe related systems.[37] Transition states were obtained by the nudged elastic band[38] and Dimer[39] methods. (See the Supporting Information for details.)

To initiate the reaction, one needs to remove a H atom from the methyl group of our model compound. This can be done either via keto−enol tautomerization or through dehydrogenation. The initial step of tautomerization has a barrier of 2.15 eV (Figure S4), whereas the dehydrogenation has a barrier of merely 1.61 eV (Figure 3a). This gives a Boltmann factor

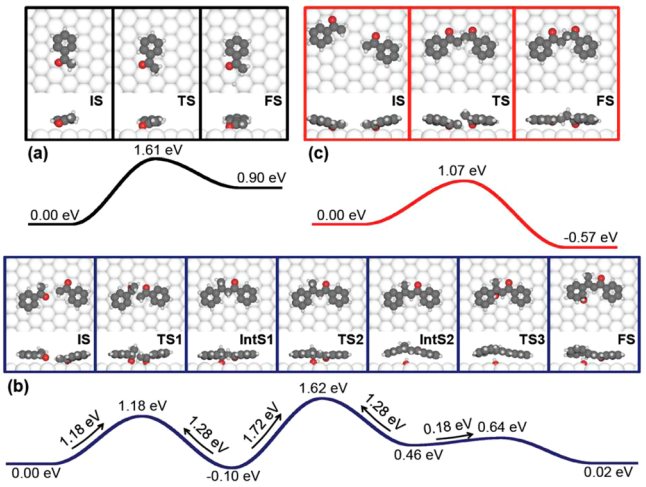

Figure 3. DFT calculations of the reaction pathways with corresponding energy profiles. (a) Dehydrogenation of a TAPB monomer. (b) Coupling between an intact and a dehydrogenated molecule. (c) Coupling between two dehydrogenated molecules.

between dehydrogenation and tautomerization of exp(0.54 eV/k_BT), which at 250 °C equals 1.6×10^5. Thus, it is safe to say that the overall reaction process is initiated by a dehydrogenation step significantly different from the mechanism in solution[30,31] so the tautomerization was not investigated further. The dehydrogenation is possible because of the chemical bond formed between the surface and the formed methyl group in the final state, avoiding an unfavorable radical intermediate species.

Two different processes were considered for the coupling between two molecules. In the first, a dehydrogenated molecule reacts with an intact one (Figure 3b). The barrier for coupling the two molecules is 1.18 eV (**IS** to **IntS1**). However, the rate-limiting step of the reaction is the second one (**IntS1** to **IntS2**), where a H and O are split-off as a hydroxyl group. Because the barrier of this second step is considerably larger than the reverse step (going from **IntS1** to **IS**, compare 1.72 to 1.28 eV), a dehydrogenated and intact molecule are required to couple and decouple numerous times before reaching **IntS2**. The transition from **IntS2** to **FS** is merely the diffusion of the hydroxyl group on the surface, which has a barrier considerably smaller than the reverse step from **IntS2** to **IntS1**. The recombination of the hydroxyl group with the dimer (**IntS2** to **IntS1**) is very unlikely. Thus, once reaching **IntS2** the process is considered irreversible.

As an alternative acetyl dimerization process, two dehydrogenated molecules may couple (Figure 3c) with a barrier of 1.07 eV, slightly smaller than the coupling of a dehydrogenated molecule with an intact one. However, this type of coupling requires a sufficient amount of dehydrogenated molecules compared to intact ones. Furthermore, the reverse barrier to breakup the dimer is just 1.64 eV, comparable to the dehydrogenation barrier of the monomer. Thus, we may question the stability of this dimer under experimental reaction conditions. Moreover, **FS** in Figure 3c is not acceptable for regular covalent networks because it does not provide the possibility for further formation of additional phenyl rings, as shown in Scheme 1b.

Importantly, in the first pathway, an intact molecule and a dehydrogenated one couple with the removal of a hydroxyl group so that an increase of C−O ratio can be expected. For the coupling between dehydrogenated molecules, there are no rest products, except for hydrogen, and this reaction should therefore result in an unchanged C−O ratio. Thus, by monitoring the C−O ratio in XPS we should be able to determine the preferred reaction pathway experimentally. We obtained the C 1s and O 1s spectra both after room-temperature deposition and 300 °C annealing (Figure 4).

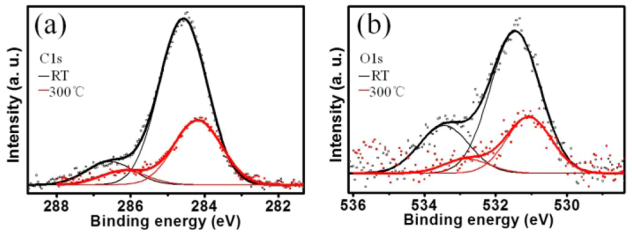

Figure 4. XPS data before and after the reaction. (a) C 1s scan of the sample. (b) O 1s scan of the sample. Black and red curve represents the signal after room temperature deposition and 300 °C annealing.

The distinct peak shifts for both C 1s and O 1s suggest a structural evolution after annealing (see Supporting Information for details). Additionally, we calculated the area covered by each spectrum, which gives the number of the C and O atoms. We found that the C−O ratio after room temperature deposition is 80 ± 2% of the ratio after annealing. Considering that the C−O ratio of pristine TAPB monomer is 10, we get the mean ratio of the product is around 12.5, which is reasonable based on the simple estimation (Figure S5). The increase and the reasonable value of the C−O ratio upon annealing strongly suggests that the proposed mechanism in Figure 3b does occur during the surface reaction. However, one still can not 100% rule out the possibility of the mechanism shown in Figure 3c. Though the mechanism shown in Figure 3c cannot contribute to the regular 2D networks formation, it may be involved during the formation of numerous defects (Figure 1d) with a certain probability.

It is worth noting that upon increased coverage the conjugated polymer structure covers almost the entire surface (Figure S6) and a second layer is not observed. Although the orientation of the polymers is not perfectly aligned, one may still expect unique transport properties because electrons can sufficiently move within this large scale covalently connected networks. In addition, we find such reaction is quite universal for other metal substrates, e.g., Au(111) and Cu(111) (Figure S7). It turned out that the covalent networks on Ag surface are

DOI: 10.1021/jacs.5b00774
J. Am. Chem. Soc. 2015, 137, 4904−4907

most regular (Figure S7), similar to what has been observed for the on-surface Ullmann coupling[8] (see Supporting Information for details).

In summary, we reported a new type of surface-assisted chemical reaction, which synthesizes 2D covalent networks by cyclotrimerization of trifunctional acetyl compounds. The reaction is carefully studied by STM, capturing numerous types of products, involving the elongated linear structure with zigzag shape and the extended graphenelike networks. Aided by DFT calculations and XPS measurements, we explored plausible reaction mechanisms, distinguishing the rate-limiting steps of the reaction and the side products. Considering the high reaction-site selectivity, we envision that by rational design of the acetyl-containing monomers, one may realize large-scale surface covalent organic frameworks.

■ ASSOCIATED CONTENT

Supporting Information

Self-assembly and reaction behavior on different substrates, temperature and coverage dependent experiments, and DFT calculations. This material is available free of charge via the Internet at http://pubs.acs.org.

■ AUTHOR INFORMATION

Corresponding Authors

*chilf@suda.edu.cn
*liqing@suda.edu.cn

Notes

The authors declare no competing financial interests.

■ ACKNOWLEDGMENTS

We thank Prof. D. H. Yan and Prof. H. B. Wang for the XPS measurements. This work was supported by the NSFC (nos. 91227201 and 21403149) and Major State Basic Research Development Program of China (no. 2014CB932600). We acknowledge the Collaborative Innovation Center of Suzhou Nano Science and Technology. Computational resources were allocated at the National Supercomputer Centre, Sweden, through SNAC.

■ REFERENCES

(1) Yang, L. Y. O.; Chang, C. Z.; Liu, S. H.; Wu, C. G.; Yau, S. L. *J. Am. Chem. Soc.* **2007**, *129*, 8076−8077.
(2) Grill, L.; Dyer, M.; Lafferentz, L.; Persson, M.; Peters, M. V.; Hecht, S. *Nat. Nanotechnol.* **2007**, *2*, 687−691.
(3) Gourdon, A. *Angew. Chem., Int. Ed.* **2008**, *47*, 6950−6953.
(4) Treier, M.; Richardson, N. V.; Fasel, R. *J. Am. Chem. Soc.* **2008**, *130*, 14054−14055.
(5) Weigelt, S.; Busse, C.; Bombis, C.; Knudsen, M. M.; Gothelf, K. V.; Lægsgaard, E.; Besenbacher, F.; Linderoth, T. R. *Angew. Chem., Int. Ed.* **2008**, *47*, 4406−4410.
(6) Matena, M.; Riehm, T.; Stöhr, M.; Jung, T. A.; Gade, L. H. *Angew. Chem., Int. Ed.* **2008**, *47*, 2414−2417.
(7) Perepichka, D. F.; Rosei, F. *Science* **2009**, *323*, 216−217.
(8) Bieri, M.; Nguyen, M. T.; Gröning, O.; Cai, J. M.; Treier, M.; Aït-Mansour, K.; Ruffieux, P.; Pignedoli, C. A.; Passerone, D.; Kastler, M.; Müllen, K.; Fasel, R. *J. Am. Chem. Soc.* **2010**, *132*, 16669−16676.
(9) Sun, Q.; Zhang, C.; Kong, H. H.; Tan, Q. G.; Xu, W. *Chem. Commun.* **2014**, *50*, 11825−11828.
(10) Li, Q.; Owens, J. R.; Han, C. B.; Sumpter, B. G.; Lu, W. C.; Bernholc, J.; Meunier, V.; Maksymovych, P.; Fuentes-Cabrera, M.; Pan, M. H. *Sci. Rep.* **2013**, *3*, 2102.
(11) Fan, Q. T.; Wang, C. C.; Han, Y.; Zhu, J. F.; Hieringer, W.; Kuttner, J.; Hilt, G.; Gottfried, J. M. *Angew. Chem., Int. Ed.* **2013**, *52*, 4668−4672.
(12) Nitzan, A.; Ratner, M. A. *Science* **2003**, *300*, 1384.
(13) Lipton-Duffin, J. A.; Ivasenko, O.; Perepichka, D. F.; Rosei, F. *Small* **2009**, *5*, 592−597.
(14) Cai, J. M.; Ruffieux, P.; Jaafar, R.; Bieri, M.; Braun, T.; Blankenburg, S.; Muoth, M.; Seitsonen, A. P.; Saleh, M.; Feng, X. L.; Müllen, K.; Fasel, R. *Nature* **2010**, *466*, 470−473.
(15) Linden, S.; Zhong, D.; Timmer, A.; Aghdassi, N.; Franke, J. H.; Zhang, H.; Feng, X.; Müllen, K.; Fuchs, H.; Chi, L.; Zacharias, H. *Phys. Rev. Lett.* **2012**, *108*, 216801−216806.
(16) Chen, Y. C.; de Oteyza, D. G.; Pedramrazi, Z.; Chen, C.; Fischer, F. R.; Crommie, M. F. *ACS Nano* **2013**, *7*, 6123−6128.
(17) Narita, A.; Feng, X. L.; Hernandez, Y.; Jensen, S. A.; Bonn, M.; Yang, H. F.; Verzhbitskiy, I. A.; Casiraghi, C.; Hansen, M. R.; Koch, A. H. R.; Fytas, G.; Ivasenko, O.; Li, B.; Mali, K. S.; Balandina, T.; Mahesh, S.; De Feyter, S.; Mullen, K. *Nat. Chem.* **2014**, *6*, 126−132.
(18) Zhang, Y. Q.; Kepčija, N.; Kleinschrodt, M.; Diller, K.; Fischer, S.; Papageorgiou, A. C.; Allegretti, F.; Björk, J.; Klyatskaya, S.; Klappenberger, F.; Ruben, M.; Barth, J. V. *Nat. Commun.* **2012**, *3*, 1286−1293.
(19) Eichhorn, J.; Heckl, W. M.; Lackinger, M. *Chem. Commun.* **2013**, *49*, 2900−2902.
(20) Zhang, X. M.; Liao, L. Y.; Wang, S.; Hu, F. Y.; Wang, C.; Zeng, Q. D. *Sci. Rep.* **2014**, *4*, 3899.
(21) Otero, G.; Biddau, G.; Sánchez, C.; Caillard, R.; López, M. F.; Rogero, C.; Palomares, F. J.; Cabello, N.; Basanta, M. A.; Ortega, J.; Méndez, J.; Echavarren, A. M.; Pérez, R.; Gómez-Lor, B.; Martin-Gago, J. A. *Nature* **2008**, *454*, 865.
(22) Treier, M.; Pignedoli, C. A.; Laino, T.; Rieger, R.; Müllen, K.; Passerone, D.; Fasel, R. *Nat. Chem.* **2011**, *3*, 61−67.
(23) Zhong, D. Y.; Franke, J. H.; Podiyanachari, S. K.; Blömker, T.; Zhang, H. M.; Kehr, G.; Erker, G.; Fuchs, H.; Chi, L. F. *Science* **2011**, *334*, 213−216.
(24) Liu, X. H.; Guan, C. Z.; Ding, S. Y.; Wang, W.; Yan, H. J.; Wang, D.; Wan, L. J. *J. Am. Chem. Soc.* **2013**, *135*, 10470−10474.
(25) Schmitz, C. H.; Ikonomov, J.; Sokolowski, M. *J. Phys. Chem. C* **2011**, *115*, 7270−7278.
(26) Liu, J.; Ruffieux, P.; Feng, X. L.; Müllen, K.; Fasel, R. *Chem. Commun.* **2014**, *50*, 11200−11203.
(27) Zhou, H. T.; Liu, J. Z.; Du, S. X.; Zhang, L. Z.; Li, G.; Zhang, Y.; Tang, B. Z.; Gao, H. J. *J. Am. Chem. Soc.* **2014**, *136*, 5567−5570.
(28) Liu, J. Z.; Lam, J. W. Y.; Tang, B. Z. *Chem. Rev.* **2009**, *109*, 5799−5867.
(29) Dong, H. C.; Zheng, R. H.; Lam, J. W. Y.; Häussler, M.; Qin, A.; Tang, B. Z. *Macromolecules* **2005**, *38*, 6382.
(30) Zhao, Y.; Li, J.; Li, C.; Yin, K.; Ye, D.; Jia, X. *Green Chem.* **2010**, *12*, 1370−1372.
(31) Rose, M.; Klein, N.; Senkovska, I.; Schrage, C.; Wollmann, P.; Böhlmann, W.; Böhringer, B.; Fichtner, S.; Kaskel, S. *J. Mater. Chem.* **2011**, *21*, 711−716.
(32) Bieri, M.; Treier, M.; Cai, J. M.; Aït-Mansour, K.; Ruffieux, P.; Gröning, O.; Gröning, P.; Kastler, M.; Rieger, R.; Feng, X. L.; Müllen, K.; Fasel, R. *Chem. Commun.* **2009**, *45*, 6919−6921.
(33) Kresse, G.; Furthmüller, J. *Phys. Rev. B* **1996**, *54*, 11169.
(34) Dion, M.; Rydberg, H.; Schröder, E.; Langreth, D. C.; Lundqvist, B. I. *Phys. Rev. Lett.* **2004**, *92*, 246401.
(35) Thonhauser, T.; Cooper, V. R.; Li, S.; Puzder, A.; Hyldgaard, P.; Langreth, D. C. *Phys. Rev. B* **2007**, *76*, 125112.
(36) Hamada, I. *Phys. Rev. B* **2014**, *89*, 121103.
(37) Björk, J.; Stafström, S. *ChemPhysChem* **2014**, *15*, 2851−2858.
(38) Henkelman, G.; Uberuaga, B. P.; Jónsson, H. *J. Chem. Phys.* **2000**, *113*, 9901−9904.
(39) Kästner, J.; Sherwood, P. *J. Chem. Phys.* **2008**, *128*, 014106.

DOI: 10.1021/jacs.5b00774
J. Am. Chem. Soc. 2015, 137, 4904−4907